ROSE 2013 - IEEE International Symposium on Robotic and Sensors Environments
Washington, DC, 21-23 October 2013

Tendon Transmission Efficiency of A Two-finger Haptic Glove

Zhou MA, Pinhas Ben-Tzvi
Robotics and Mechatronics Lab (RML)
Department of Mechanical & Aerospace Engineering
The George Washington University
Washington DC, United States
{mazhou, bentzvi}@gwu.edu

***Abstract*—This paper presents a two-fingered haptic interface named RML-glove. With this system, the operator can feel the shape and size of virtual 3D objects, and control a robot through force feedback. The tendon driven system makes this haptic glove a lighter and portable system that fits on a bare hand, and adds a haptic sense of force feedback to the fingers without constraining their natural movement. In order to explore the effect of cable friction and frictional losses in this system, experiments were conducted to investigate the impact of different variables including pulleys' active arc, tendon velocity, as well as cable tension and lubrication.**

Keywords—haptic glove; link length; optimization; inverse kinematics; workspace

I. INTRODUCTION

The glove discussed in this paper provides haptic feedback during bidirectional human–robot interaction. Haptic interfaces can measure the user's hand movement, while concurrently providing the operators with force and torque information generated from a remote environment. During the last decade, haptic devices have been utilized in many applications of medical training and rehabilitation [1-3], tele-surgery [4-7], tele-manipulation, tele-navigation [8], as well as micromanipulation [9].

Among a variety of haptic devices, haptic gloves are a preferred choice for hand-motion-based control since they can provide a large array of force feedback. The high dexterity of haptic gloves also makes them applicable to the control of complex movements of remote robots, as opposed to other non-haptic devices such as joysticks. Although many research activities are performed on haptic glove designs [10-12], existing systems typically restrict the natural motion of the hand because they are bulky and heavy.

Some of the design issues concerning haptic gloves include:

- Size: which should be small enough to fit on a human hand.
- Weight: which should be light enough to enable portability on a human hand.
- Flexibility: in order to provide adequate dexterity without constraining the natural motion of a hand, thus imposing the need for sufficient degrees of freedom.

The goal of this research is to provide a haptic glove that satisfies these objectives, while being comfortable enough to wear and operate. As such, a bidirectional pulley-tendon system was adopted in this research to activate each finger mechanism. Thanks to this mechanism, the transmission was greatly simplified, and the following additional benefits were achieved with the RML-Glove:

- Reduction of Actuators: where every finger mechanism was actuated by one motor, thereby reducing the number of actuators without impacting the performance of the mechanism.
- Magnification of force feedback: which was accomplished via a combination of cable strength and non-back-drivability enabled by self-locking worm and worm gear assemblies.
- Amplification of workspace: which was accomplished by placing the actuators at a remote location at the back of the hand, thereby preventing the restriction of the natural motion of an anthropomorphic finger while increasing the workspace of the proposed glove.

However, the drawback of using a pulley tendon system to couple the motion of a remote motor to the motion of each finger is evident in the loss of power resulting from low transmission efficiencies. Despite the existence of some relevant friction efficiency research in the literature [13, 14], the unique design of every mechanical system imposes a unique understanding of its mechanical efficiencies. With the proposed RML-Glove, we study the particular loss of power generated by the tendon transmission by investigating the non-linear effects of Coulomb friction, viscous friction, and static friction [15]. This is done experimentally for different design variables, such as pulleys' active arc, tendon velocity, as well as cable tension and lubrication.

The paper is organized as follows: Section II describes the mechanical design and modeling of RML-Glove. Section III explains the electrical design of the system. The tendon transmission efficiency analysis and experiments are presented in section IV before concluding this paper in Section V.

978-1-4673-2939-2/13/$31.00 ©2013 IEEE

II. MECHANICAL DESIGN

A. Mechanism

The proposed RML-glove, shown in the CAD model in Fig. 1, provides a real feel of grasping applicable to all segments of every finger, and satisfies the requirements of size, weight and flexibility established in the introduction. The design incorporates a multi-link redundant serial mechanism for each finger which accommodates different hand sizes, and delivers a force magnitude that matches the human hand output force as reported in [16]. Because all necessary components are contained inside the glove, including power supplies, wireless communication and on-board processing, the user can move freely around without being restricted by a tethered cable.

Fig. 2 shows the two-finger prototype of the RML-Glove. Each finger has three joints and four degree of freedoms (DOFs). This configuration follows the model of human physiology and by recreating the joints of a human finger. In order to simplify the glove, the movements of the Distal Interphalangeal (DIP), Metacarpophalangeal (MCP) and Proximal Interphalangeal (PIP) joints of each finger are coupled together with one actuator. All joints in this design are realized through revolute pin connections. Flexion/Extension and adduction/abduction movements are possible with this mechanism.

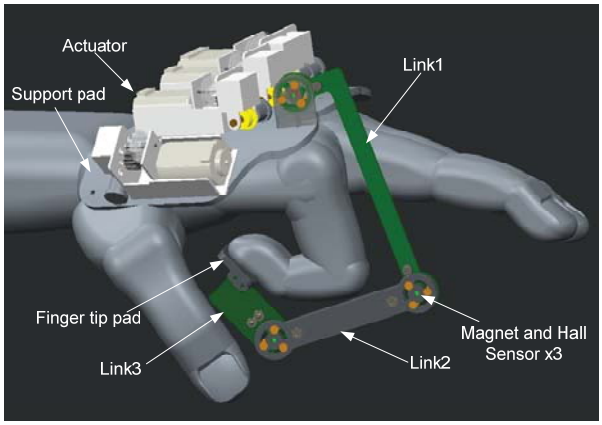

Fig. 1. CAD model of one-finger RML-Glove.

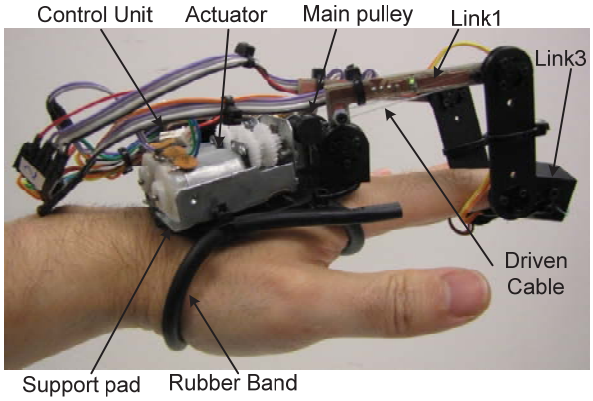

Fig. 2. Side view of a left hand wearing a two-finger RML-Glove.

The RML-Glove is further designed to fit onto the back of the hand [17], so the operator can manipulate it intuitively with a natural motion of the fingers. Three basic components define the proposed design: a support pad, two motors, and two fingers as shown in Fig. 2. The support pad is made of thermoplastic in a curved shape that matches the back profile of a human hand. This pad is secured to the hand by a length-adjustable elastic band. Electronic components, including the control system and batteries, are also attached to the support pad. The actuator unit, connected to the support pad, consists of a brushed DC-motor (Mabuchi FA-130) with a 101:1 gear ratio. The terminal stage of the gear train is a non-back drivable worm gear assembly.

The pulley that actuates each finger is directly connected to the output shaft of the motor housed on the pad at the back of the hand. Each finger mechanism is further attached to the support pad through a pin joint which enables it to swivel in the adduction/abduction direction freely. The finger also has a mechanical limit to restrain its rotational bounds. There are three links for each finger mechanism, as shown in the exploded view in Fig. 3. To minimize the link thickness and simplify the mechanical layout, Link 1 and Link 3 are manufactured from customized printed circuit boards (PCB) as shown in Fig. 4. Two angular position encoders are mounted on Link 1 to measure the angles of the first two joints. These Hall Effect encoders are soldered directly onto the PCB board which is used as both a mechanical chassis and a carrier of electrical components. This dual function makes the RML-Glove lighter without sacrificing strength. Link 2 is made of thermoplastic and connects Link 1 and Link 3 through pin joints.

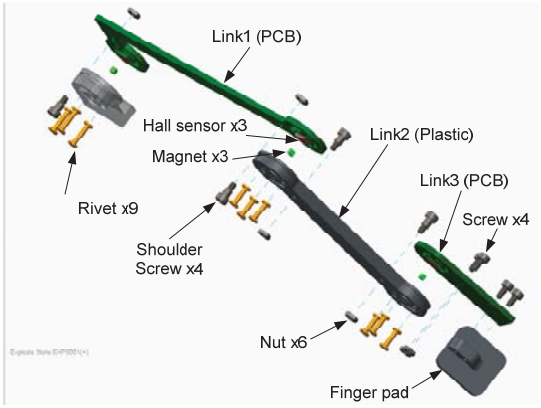

Fig. 3. Explode view of one finger mechanism

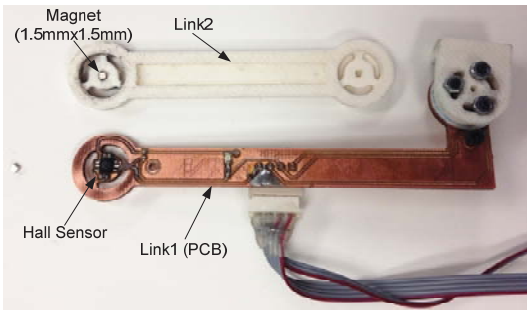

Fig. 4. Angular senssor design of the RML-Glove

B. *Actuation System*

Each finger mechanism is controlled by a pair of tendons routed through primary and secondary pulleys as shown in Fig. 5. This pulley-tendon assembly transmits torque from the motor to the finger joints. One end of the tendon is wound about the active pulley which is attached to the motor's output shaft, while the other end is attached to the tip of Link 3.

The pair of tendons is wound in opposite directions around the motor's pulley thus works as a differential mechanism. The pull-pull configuration allows transmission of force and position in both directions. Bidirectional force control is enabled by an antagonistic actuation of the tendons of each finger, transferring force along the exoskeleton to the fingertip. These forces drive the links to either follow or resist finger movement.

In such configuration, the actuator controls the relative length of the tendon, pulling one of the opposing tendon while simultaneously lengthening the other. When the actuator rotates the active pulley clockwise (Fig. 5), the grasp tendon is tensioned and the mechanism and the index finger close. When the actuator rotates counter clockwise, the release tendon is tensioned and the finger will open. The glove links allow full flexion and extension in all joints.

This mechanism doesn't have any limit in adduction/abduction direction since movement in these directions will not affect the cable length change. The material of dyneema was chosen as the tendon cable because of its great characters: high strength, light weight, low stretch and flexible.

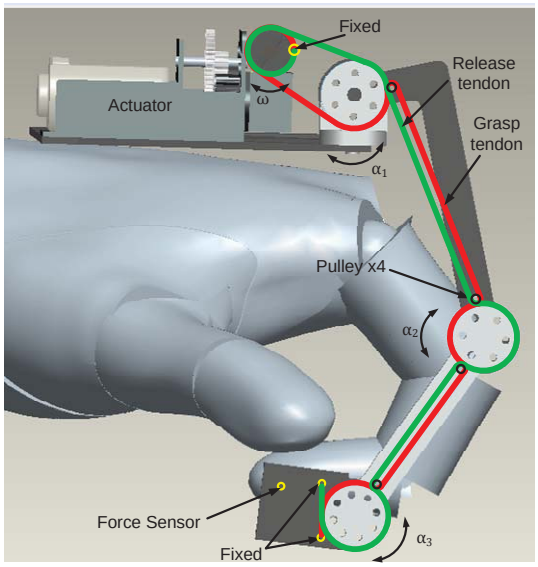

Fig. 5. Cable transmission model.

III. ELECTRICAL DESIGN

The proposed haptic device is composed of a glove skeleton and a control interface. The interface uses a MEGA168 (Atmel Corp) microcontroller to acquire force sensor data, as well as control the amount of force applied at the user's fingertips by controlling the motion of the corresponding motor. This interface also enables wireless communication between the glove and the robot.

To ensure a stable and precise force output, the loop of the control program is set to run at a frequency of 1.3 kHz, in excess of the typical 1 kHz recommended for haptic devices. This high cycle frequency provides both realistic touch feelings to the user of the haptic glove, while helping to maintain the control stability of the entire system.

Force Sensitive Resistor (FSR) sensors are used for force feedback. These are mounted inside the fingertip pad as shown in Fig. 5. Communication between the haptic glove and the mobile robot is accomplished through a wireless XBee 2.4GHz RF Module (1mW power, 30m working range indoor). The wireless transmission speed is 57,600 bits/second in this case, and the electrical design diagram is shown in Fig. 6. The transmitted data from the haptic glove contains finger joint angles, fingertip applied force, and input pulley speed commands for the mobile robot. The data that the haptic glove receives includes robot speed, as well as the magnitude of the forces that the glove's motors need to apply at every fingertip via the pulley-tendon mechanism.

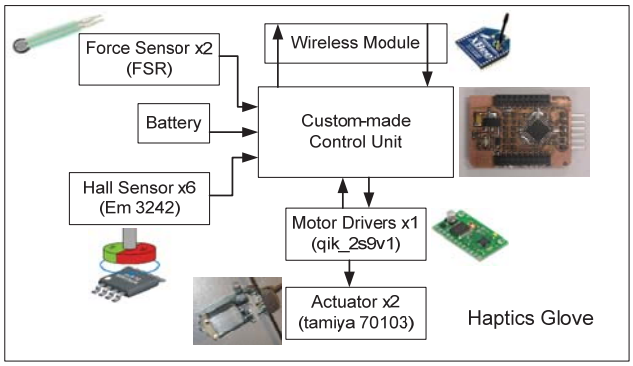

Fig. 6. Electrical design diagram.

IV. FRICTION COEFICIENT EXPERIMENT

Each finger of the RML-Glove is actuated by a motor that generates tension in a pair of tendons. The tendons are routed from the actuator to the fingertip via pulleys. However, friction between the tendons and the pulleys reduces the amount of force available at the fingertip. To compensate for this loss of power, the actuator must generate extra tension, which increases the current consumption and reduces the overall efficiency of the mechanism. As such, one of the primary objectives of this research was to experimentally analyze the transmission efficiency of the proposed glove, and to explore new venues for improvement.

In order to simplify the design and minimize the weight of RML-Glove, the secondary pulleys were made of a steel ring, as shown in Fig. 7. Thus the secondary pulley can be model as a stationary cylinder (shown in Fig. 8). Furthermore, since the tendons wrap around the cylinder at a given angle γ, the relationship between the forces applied at both ends of the pulley can be modeled using the belt friction model [18]:

$$\frac{F_1}{F_2} = e^{\mu\gamma} \tag{1}$$

where F_1 is the active pulling force, F_2 is the passive force, μ is the coefficient of kinetic friction between the tendon and the pulley, and γ is the wrap angle measured in radians. As (1) indicates, the main parameters influencing the performance of the cable transmission are the total wrap angle γ and the friction coefficient μ generated between the tendons and the pulleys, whereas the pulley's radius and the velocity of the tendons do not play a role in this efficiency.

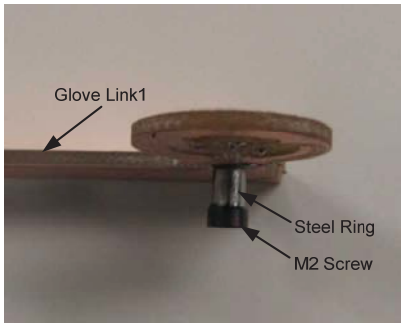

Fig. 7. Secondary pulley.

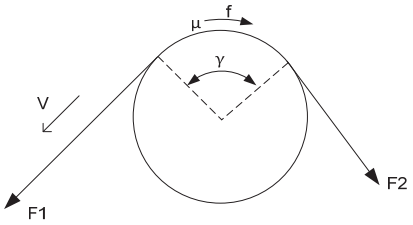

Fig. 8. Free body diagram of the pulley.

A. *Experimental set- up*

Fig. 9 shows the apparatus used to analyze the friction coefficient between the tendons and the pulleys. To experimentally study the tension over the fixed secondary pulley, a weight was suspended from one end of the tendon. In order to eliminate the static friction effect, a 50W brushless motor with a 23:1 planetary gearbox (maxon Gear 166936, maxon motor 251601) was attached to the other end of the tendon; lifting and lowering the weight at a constant speed. A load cell (MLP-10, Transducer Techniques, Inc) was connected in series with the tendon between the motor and the pulley to measure the tension force applied to the tendon. This apparatus was used in a series of experiments to measure the friction coefficient under both lubricated and non-lubricated conditions.

First, the wrap angle was varied from 0 to 315° in a 45° increment to evaluate its effect on friction coefficient. Second, the effect of the external load on the performance of the glove tension system was investigated. The weight at the end of the tendon was varied from 100g to 1kg in 100g increments. Different tendon moving velocities were also tested, with the motor output speed varied from 10 rpm to 100rpm to generate a tendon moving velocity between 2mm/s and 20mm/s. Finally, different lubrication conditions were tested to evaluate their effect on the friction coefficient. Note that the force measured by the load cell during the lifting process corresponds to the active pulling force defined by in (1). On the other hand, when the actuator lowers the weight, the load cell measures the passive pulling force defined by in (1).

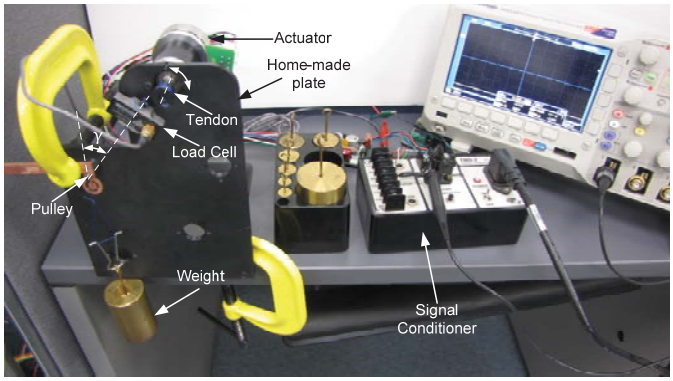

Fig. 9. Experimental set up for analyzing the transmission efficiency of the proposed tendon-based RML-glove

B. *Results and discussion*

Fig. 10 and Fig. 11 depict the load cell output for various weights and different wrap angles under both lubricated and none-lubricated conditions. From the experimental data, the friction coefficient can be easily found by applying a least-squares curve fitting, and the results were plotted in Fig. 12.

Apparently, the friction coefficient data at 45 degree varies the other larger angles too much in both lubricated and non-lubricated conditions. And in the RML-Glove system, the wrap angle is around 100-150 degree. So the 45-degree data was removed and the average non-lubricated friction coefficient is 0.0631. And the average lubricated friction coefficient is 0.0530.

Tendon efficiency is defined as the ratio of the output tension to the input tension (F_1/F_2). Using the friction coefficients μ and μ' with (1), the efficiency of the tendon with and without lubricant in the RML-Glove is plotted against the wrap angle in Fig. 13. This figure shows that lubrication has a higher impact at greater wrap angles. With a 90° wrap angle, the lubricated tendon efficiency was only 1% better than the none-lubricated efficiency. With a 360° wrap angle, the lubricated system was 5% more efficient. In this research, the wrap angle of the secondary pulley is less than 360°, so the lubricated condition does not exhibit a great impact on the tendon efficiency (less than 5%). However, in order to reduce the wear of the tendons, lubrication was employed. Another benefit of lubrication is that it allows the mechanism to run smoother under continuous operation with only mild wear, and without excessive stress or seizure at the pulleys.

Different tendon velocities were also investigated. With a wrap angle of 90°, and with a weight of 1 Kg in the lubricated condition, the experimental results are shown in Fig. 14. These results prove that the tendon velocity does not influence the tendon friction.

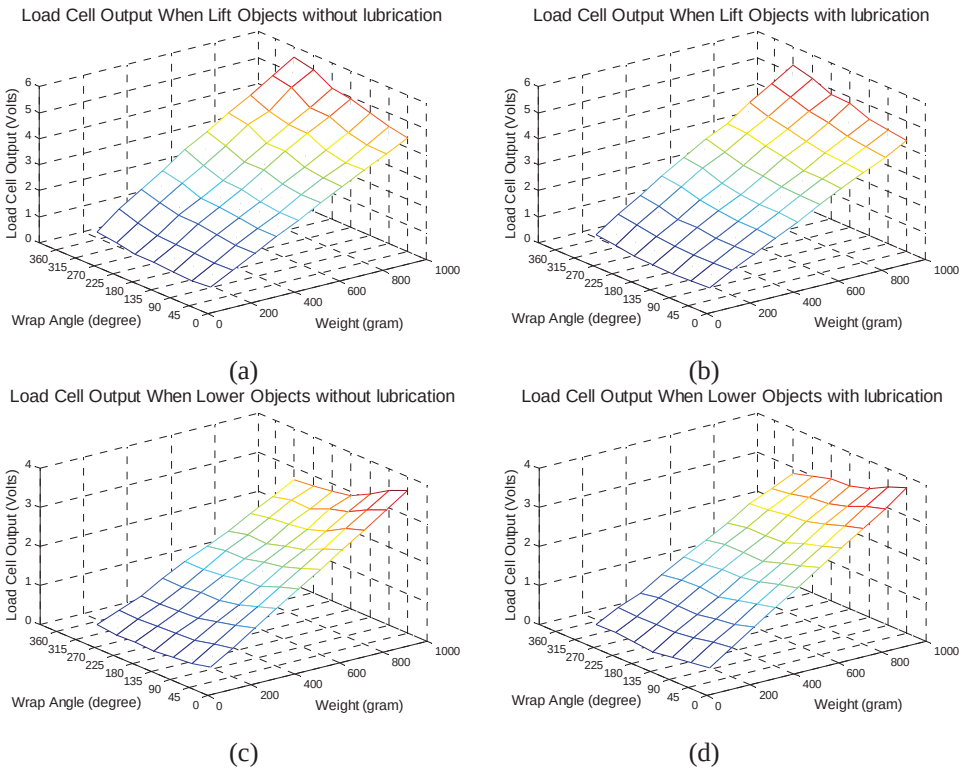

Fig. 10. Load cell output plots.

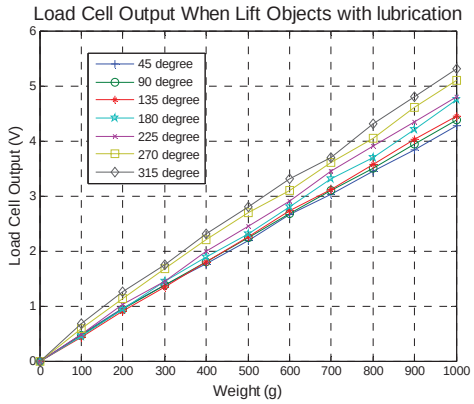

Fig. 11. Load cell output least-squares fitting plots.

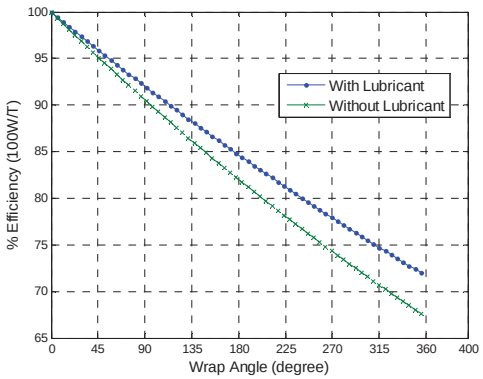

Fig. 13. Force transmission efficiency in RML-Glove cable system.

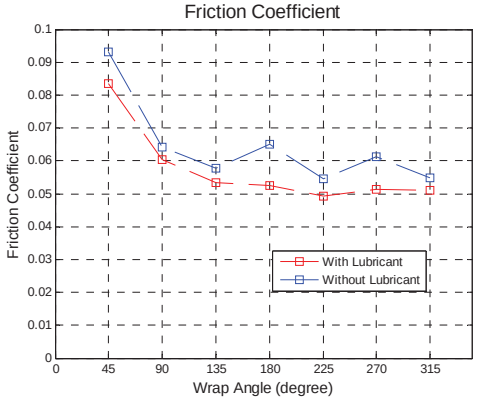

Fig. 12. Load cell output with and without lubrication.

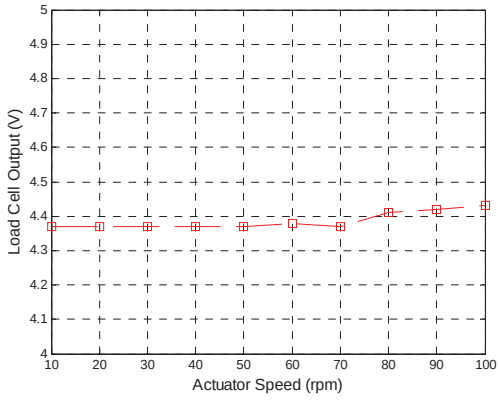

Fig. 14. Force transmission efficiency in RML-Glove cable system.

V. CONCLUSION

In this paper, a method for sensor-based haptic gloves is presented. The haptic device is a lightweight and portable actuator system that fits on a bare hand and adds tactile force feedback to each finger of the hand without constraining the natural movement of the fingers. The proposed multi-link mechanism is suitable for multiple finger operation and has a large workspace. Cable transmission is chosen because it can provide adequate power transmission through narrow pathways while allowing the actuator to be located at a distance from the fingers. Since a cable can only be used in tension, for an n-DOF system, 2n cables are required. Therefore, a two-cable pull-pull transmission was adopted and actuated with one brushed DC motor located at the back of the hand.

In order to explore the effects of the friction coefficient and other variables on the efficiency of the mechanism, three experiments were conducted, and different variables were investigated including tendon wrap angle, tendon velocity, the amount of tension in the cables, and the lubrication condition.

In the future, a full five-finger glove will be integrated. This system will employ all anthropomorphic fingers with sufficient dexterity to control the navigation and manipulation of a mobile robot.

REFERENCES

[1] C. Basdogan, C. H. Ho, and M. A. Srinivasan, “Virtual environments for medical training: Graphical and haptic simulation of laparoscopic common bile duct exploration,” IEEE/ASME Trans. echatron., vol.6,no. 3, pp. 269–286, Sep. 2001.

[2] Mao, Y. and Agrawal, S. K., “Design of a Cable Driven Arm Exoskeleton (CAREX) for Neural Rehabilitation”, IEEE Transactions on Robotics, Vol. 28, No. 4, 2012, 922-931.

[3] N. A. Langrana, G. Burdea, K. Lange, D. Gomez, and S. Deshpande, “Dynamic force feedback in a virtual knee palpation,” Artif. Intell. Med., vol. 6, pp. 321–333, 1994.

[4] I. Ivanisevic and V. J. Lumelsky, “Configuration space as a means for augmenting human performance in teleoperation tasks,” IEEE Trans. Syst., Man Cybern. B, vol. 30, no. 3, pp. 471–484, Jun. 2000.

[5] R. V. Dubey, S. E. Everett, N. Pernalete, and K. A. Manocha, “Teleoperation assistance through variable velocity mapping,” IEEE Trans. Robot. Autom., vol. 17, no. 5, pp. 761–766, Oct. 2001.

[6] I. Elhajj, N. Xi, W. K. Fung, Y. H. Liu, W. J. Li, T. Kaga, and T. Fukuda, “Haptic information in internet-based teleoperation,” IEEE/ASME Trans. Mechatron., vol. 6, no. 3, pp. 295–304, Sep. 2001.

[7] N. Ando, P. Korondi, and H. Hashimoto, “Development of micromanipulator and haptic interface for networked micromanipulation,” IEEE/ASME Trans. Mechatron., vol. 6, no. 4, pp. 417–427, Dec. 2001.

[8] O. D. Gabriel Sepulveda, Vicente Parra. “Haptic cues for effective learning in 3d maze navigation”, IEEE International Workshop on Haptic Audio Visual Environments and Games, Ottawa.Canada, October 2008.

[9] M. Guthold, M. R. Falvo, W. G. Matthews, S. Paulson, S. Washburn, D.A. Erie, R. Superfine, F. P. Brooks, Jr., and R.M. Tylor, “Controlled manipulation of molecular samles with the nanomanipulator,” IEEE/ASME Trans. Mechatron., vol. 5, no. 2, pp. 189–198, Jun. 2000

[10] M. Turner, D. Gomez, M. Tremblay, and M. Cutkosky, “Preliminary tests of an arm-grounded haptic feedback device in telemanipulation,” in Proc. ASME WAM, vol. DSC-64, 1998, pp. 145–149.

[11] Blake, J. and Gurocak, H.B. 2009. ‘‘Haptic Glove With MR Brakes for Virtual Reality,’’ IEEE/ASME Transactions on Mechatronics,Vol. 14, no. 2, October 2009.

[12] M. Bouzit, G. Burbea, G. Popescu, R. Boian, “The Rutgers Master II-New Design Force-Feedback Glove,” IEEE/ASME Trans. on Mechatronics, Vol. 7, Issue 2, 2002, pp. 256-263.

[13] L.B. Carlson, B.D. Veatch, and D. Frey. Efficiency of prosthetic cable and housing. Journal of Prosthetics and Orthotics, 7(3):96ff, 1995.

[14] A. Schiele, "Performance Difference of Bowden Cable relocated and non-relocated master actuators in virtual environment applications", in Proc. IEEE Int. Conf. on Intelligent Robots and Systems, Nice, France, Sep 2008, pp 3507-3512

[15] A. Schiele et al., Bowden Cable Actuator for Force-Feedback Exoskeletons, In Proc. Of IEEE/RSJ Int. Conference on Intelligent Robots and Systems, 2006, pp. 3599-3604

[16] [15] Arm, Hand, and Thumb/Finger Strength. (2008). [Online]. Available: http://msis.jsc.nasa.gov/sections/section04.htm#Figure%204.9.3-4

[17] Z. MA, P. Ben-Tzvi, “An Admittance-Type Haptic Device-RML Glove”, 2011 ASME International Mechanical Engineering Congress and Exposition (IMECE 2011), Denver, CO, November 11-17, 2011.

[18] L.B. Carlson, B.D. Veatch, and D. Frey, “Efficiency of prosthetic cable and housing” Journal of Prosthetics and Orthotics, 7(3):96ff, 1995.